

HARTREE-FOCK MODEL OF A SELF-AVOIDING FLEXIBLE POLYMER

C. BOUCHIAT

*Laboratoire de Physique Théorique de l'École Normale Supérieure*¹
24, rue Lhomond, F-75231 Paris Cedex 05, France

Recent measurements of the force versus extension curves in stretched single stranded DNA, under conditions where the hydrogen bonding between complementary bases is inhibited, provide a new handle for the study of self-avoiding effects in a flexible polymer. We report in this paper upon analytic computations of the force versus extension curves within a continuous version of the freely joining chain model, with monomer-monomer repulsive interactions. The problem is formulated as a Statistical Field Theory model, endowed with a fixed cutoff associated with the curvature of the extension versus force curve, in the free polymer limit. Using a Field Theory version of the Hartree-Fock approximation, the self-avoiding single polymer problem reduces to the solving of a one-dimension self-consistent integral equation. Taking the short range potential limit, we obtain an explicit analytical solution, involving the roots of an algebraic equation. In the low force regime, we find that the slope of the relative extension at zero force increases steadily with the total monomer number N , while it stays constant for a free polymer. We compare, for $N = 100$, our analytic results with those obtained by Monte Carlo simulations of a discrete freely joining chain, in presence of excluded volume effects. Despite a difference between the repulsive potential ranges d , an appropriate choice of our single free parameter leads to a good agreement between the two computations. This may be considered as an indication that the shape of the extension curve is not very sensitive to d , if it is equal to or less than the monomer length.

¹UMR 8549: Unité Mixte du Centre National de la Recherche Scientifique et de l'École Normale Supérieure

PACS numbers: 87.15 By, 61.41.+e

Introduction and Summary

During the last few years, the elastic properties of single biopolymer molecules, under physical conditions close to those encountered in living organisms, have been the subject of extensive investigations [1, 2, 3]. In particular, the force versus extension curves of double stranded DNA (dsDNA) have been measured accurately within a wide range of pulling forces. In absence of supercoiling constraints, the entropic elasticity of the dsDNA molecule is very well described [4] by an elastic string [5] model, the so-called Worm Like Chain (WLC) model, involving a single rigidity associated with the resistance against the polymer bending. The dsDNA persistence length A is given, within the WLC model, by the bending rigidity written with appropriate units. Micromanipulations experiments lead to values clustering around $A \simeq 50 \text{ nm}$, which corresponds to 150 base pairs, hence the qualification "stiff" polymer sometimes given to the dsDNA. The monomer-monomer interactions in dsDNA are dominated by the screened Coulomb repulsion and they do not seem to lead to significant corrections to the WLC model predictions[6], with the exception of very long chains, longer than $50 \mu\text{m}$ [7].

There has been recently a growing interest for micromanipulation experiments [9, 10] involving the stretching of single stranded (ss)DNA. The elasticities of ssDNA and dsDNA are expected to be different, for at least two reasons. One, despite the lack of any accurate determination, it is commonly believed that the ssDNA persistence lies in the range 0.7 to 3 nm [8], corresponding roughly to a base pair number between 2 and 7. In presence of thermal fluctuations, the molecular local axis loses the memory of its direction after few base pairs. We express this fact by saying that the ssDNA is a "locally flexible" polymer". In such a case, the WLC model does not lead to an adequate description of the "free" ssDNA molecular chain. A more realistic picture is provided by the freely joining chain (FJC) model, where the relative direction of two adjacent elementary links is allowed to fluctuate freely. As a consequence of the ssDNA high flexibility, the self avoiding-effects are expected to be more important than in the case of a "stiff" polymer like dsDNA, if the physical environment is such that the range of the repulsive monomer-monomer interaction is about few nm . The second reason for a difference between the ssDNA and dsDNA entropic elasticities is obviously the attractive interaction between complementary bases, leading to the so-called "hairpin" structures which have to be opened up in order to stretch the molecular chain. A theoretical analysis of this mechanism has been performed recently [11], with the help of the "rainbow" approximation. The results are in good agreement with the observations of ref.[10] when the buffer solution contains cations which stabilize the hairpin structures.

Conversely, ssDNA stretching experiments [10] have been performed under physical conditions where hydrogen bonding interactions between complementary bases are suppressed, leaving the screened Coulomb repulsion as the dominant monomer-monomer interaction. The necessity of accounting properly for self-avoiding effects appears clearly from the lack of agreement between the experimental data and the ideal polymer model predictions, like the FJC model. This is confirmed [10] by a Monte-Carlo (MC) simulation of the force vs extension curves within a FJC model with excluded volume effects.

In this paper, we compute, by Statistical Field Theory methods, the entropic elasticity of locally flexible polymers in presence of repulsive monomer-monomer interactions.

As a first step (section 1), we have constructed a continuous version of the FJC model, taking the monomer number n as the running variable along the chain. It is well known[6] that one can map the free polymer problem upon a single particle quantum problem in an Euclidian space-time. In the present case, the imaginary time is just $-i \times n$. The partition function matrix, relative to arbitrary states of the molecule free ends, is given by $\hat{Z} = \exp -N \hat{H}_0$, where \hat{H}_0 is the Hamiltonian of the attached quantum problem and N the total monomer number. In the case of the continuous version of FJC model, the Hamiltonian is purely kinetic in the zero force limit: $\hat{H}_0 = h_0 \left(\hat{\vec{p}}^2 \right)$, where $\hat{\vec{p}} = -i \vec{\nabla}$ is the momentum operator conjugated to the vector $\vec{r} = \vec{r}_N - \vec{r}_0$, joining the two ends of the chain. The force stretching energy $-\vec{r} \cdot \vec{F}$ is then implemented through the replacement: $\hat{\vec{p}} \rightarrow \hat{\vec{p}} - i\vec{F}$. One proves easily the following simple relation between the relative extension vs force function $\zeta_0(F)$ and the fictitious free particle Hamiltonian: $\zeta_0(F) = 2F h'_0(-F^2)$. In principle, the Hamiltonian \hat{H}_0 is then obtained by integrating the extension vs force function along a finite interval along the imaginary F axis. Unfortunately, the things are not so simple since $\zeta_{FJC}(F)$ has poles along integration path. We have been able to bypass this difficulty by building a function $\zeta_r(F)$ regular along the imaginary F axis and differing from $\zeta_{FJC}(F)$ by less than a few % along the whole real F axis. The coincidence is even better than 1% in the low to medium force regime where the self-avoiding effects are the most important. The Hamiltonian \hat{H}_0 is written finally as $\hat{H}_0^r = h_0^r \left((\hat{\vec{p}} - i\vec{F})^2 \right)$ where and $h_0^r(p^2)$ is an analytic function of p increasing faster than p^4 . In our construction, the quartic expansion $h_0^{(4)}(p^2) = \frac{b^2 p^2}{6} + \frac{b^2 p^4}{180}$ is in fact obtained by integrating the cubic expansion of $\zeta_{FJC}(F)$, where b is the length of the FJC elementary link. The quadratic term corresponds to the Gaussian model; when it is used in association with a short range (Dirac δ function) monomer-monomer repulsive interaction, it is called the Edwards model. The quartic terms provides a natural cutoff $\Lambda = 30b^{-2}$ for the divergences appearing in the perturbation expansion of the Edwards model with respect to the monomer-monomer interactions. It will

turn out that in the exploration of the low to medium force range $0 \leq \beta F b \leq 1.5$ the quartic Hamiltonian $h_0^{(4)}(p^2)$ can be substituted to $h_0^r(p^2)$, allowing for analytic computations.

In section 2 we develop an Hartree-Fock treatment of self-avoiding effects within our continuous version of the FJC model. With the help of a well known functional integral identity[13], the self-avoiding polymer problem is *exactly* mapped into that of a quantum single particle moving in a stochastic imaginary potential, described by the Hamiltonian: $\hat{H}^r = \hat{H}_0^r + i g \phi(\vec{r})$. The functional probability measure of the field $\phi(\vec{r})$ is of the Gaussian type, specified by the two fields product average: $\langle \phi(\vec{r}_1) \phi(\vec{r}_2) \rangle_\phi = V(|\vec{r}_1 - \vec{r}_2|)$ where $g^2 V(|\vec{r}_1 - \vec{r}_2|)$ is the repulsive monomer-monomer potential. The partition function of the self-avoiding polymer with fixed free ends is given by the stochastic field average: $Z(\vec{r}_N - \vec{r}_0, \vec{F}, N) = \langle r_N^r | \langle \exp -N (\hat{H}_0^r + i g \phi(\vec{r})) \rangle_\phi | r_0^r \rangle$. To proceed, it is convenient to perform the Laplace transform of the partition function at zero force $Z(\vec{r}, 0, N) \rightarrow z(\vec{r}, \tau)$, where τ is the variable conjugated to N . The result takes the following simple form, $z(\vec{r}, \tau) = \langle \vec{r} | \langle (h_0^r(\vec{p}^2) + i g \phi(\vec{r}) + \tau)^{-1} | 0 \rangle_\phi$, which can be readily written as a Feynman diagram expansion in power of g^2 . It allows us to use some of the Quantum Field Theory machinery, in particular the Dyson integral equations. Following a standard procedure [12], we introduce an approximate kernel in the Dyson integral equation for the propagator. We arrive in a rather direct way to the Hartree-Fock equation which performs the exact summation of the "rainbow" diagrams. The self-consistent integral equation takes a remarkable simple form in the Fourier space. It involves then the Fourier transform $\tilde{z}(\vec{p}, \tau)$ of $z(\vec{r}, \tau)$, where \vec{p} is the momentum conjugated to the relative free end coordinate \vec{r} .

$$\frac{1}{\tilde{z}(\vec{p}, \tau)} = \frac{1}{\tilde{z}_0(\vec{p}, \tau)} + \frac{g^2}{2\pi^2} \int d^3q \tilde{z}(\vec{q}, \tau) \tilde{V}(|\vec{p} - \vec{q}|) \quad (1)$$

where $\tilde{V}(|\vec{q}|)$ is the Fourier transform of the potential $V(|\vec{r}|)$ and $\tilde{z}_0(\vec{p}, \tau)$ corresponds to the free polymer partition function.

In this exploratory paper we have used a zero range potential, proportional to a Dirac δ function. The Hartree-Fock integral equation reduces in this limit to a numerical equation. We will show that $\tilde{z}(\vec{p}, \tau)$ can be written as $(h_0^r(p^2) + \mu(\tau))^{-1}$, where the function $\mu(\tau)$ obeys the self-consistent equation: $\mu(\tau) = \tau + \frac{\lambda}{6} F(\kappa, 6\mu(\tau))$, where $\kappa = b^2 \Lambda^{-2}$ and λ a positive dimensionless constant measuring the strength of the repulsive monomer-monomer potential. In the low to medium force regime, $F(\kappa, \tau)$ is a rather simple algebraic function of τ . The extension versus vs force function $\zeta(F, N)$ for the self avoiding polymer is then obtained by taking the logarithmic derivative of the inverse Laplace transform of $(h_0^r(-F^2) + \mu(\tau))^{-1}$. The involved integral is dominated by the residues of the poles at the roots of $h_0^r(-F^2) + \mu(\tau) = 0$.

In the low force regime $0 \leq \beta F b \leq 0.5$, the computation of the extension vs force function $\zeta(F, N)$ can be performed analytically up to the very end. The final expression is not by itself very illuminating, so we have plotted a set of extension curves for a wide range of monomer number: $50 \leq N \leq 5000$. The most remarkable feature is the steady increase with N of the relative extension vs force slope at the origin ($F = 0$). This contrasts with the case of a free polymer where this quantity is independent of N . This behaviour is also predicted in the Edwards model using scaling arguments[16], but the effect is notably smaller than in our approach. Such a difference was to be expected since Renormalization Group methods cannot be applied to our model which is endowed with a fixed cut-off, associated with the extension vs force curvature of the free polymer.

The section 4 is devoted to a comparison of the analytical results of our Hartree-Fock method with those obtained by a MC simulation [10] of a discrete freely joining chain, with excluded volume effects. In both cases, the total number N of monomer is one hundred. Our analytic treatment is strictly valid in the low to medium force range $0 \leq \beta F b \leq 1.5$, but we have extended our results to higher forces with the help of a reasonably safe extrapolation procedure. We are able in this way to reach the force domain, $\beta F b \geq 3.5$, where self-avoiding effects are disappearing. An appropriate choice of our single adjustable parameter, $\lambda = 0.7$, leads to a predicted extension vs force curve which is in remarkable agreement with the MC simulations. It should be stressed that there is a notable difference between the physical inputs in the two approaches. In our exploratory computation, we use a zero range potential while the MC simulations were performed with an excluded volume radius d equal to the monomer length b . This may suggest that the shape of the extension vs force curve is not very sensitive the value d of the repulsive potential range if $d \leq b$.

1 A continuous formalism for a free flexible polymer.

In this paper, the partition function for a stretched "locally flexible polymer" will be given, in absence of self-avoiding effects, by the following path integral:

$$\begin{aligned}
 Z_0(\vec{r}_N, \vec{r}_0, \vec{F}) &= \int \mathcal{D}[\vec{r}] \exp - \int_0^N dn \mathcal{E}_0(n) \\
 \mathcal{E}_0(n) &= \epsilon_0 \left(\left(\frac{d\vec{r}}{dn} \right)^2 \right) - \vec{F} \cdot \frac{d\vec{r}}{dn}
 \end{aligned} \tag{2}$$

where n stands for the monomer number which is treated as a continuous variable as a result of a coarse-graining of the polymer chain ; $\mathcal{E}_0(n)$ is the elastic energy per polymer written in thermal energy unit $k_B T$. The function $\epsilon_0(x)$ is assumed here to be analytic. The equation (2) could be considered as the definition of what we mean by a "locally flexible polymer" . In the literature about polymer self-avoiding effects,

the function $\epsilon_0(x)$ is often taken to be linear: $\mathcal{E}_0(n) = \frac{3}{2b^2}(\frac{d\vec{r}}{dn})^2 - \vec{F} \cdot \frac{d\vec{r}}{dn}$ where b is the root mean square distance of two adjacent polymers. The difficulty with this model-known as the "Gaussian model"- lies in the fact that the extension vs force curve turns out to be a straight line, which is quite unrealistic. The philosophy taken up in this paper is to consider as the true starting point the extension vs force function in absence of self-avoidance : $\langle z_N \rangle / N = \zeta_0(F)$, rather than the elastic energy $\epsilon_0 \left((\frac{d\vec{r}}{dn})^2 \right)$ appearing in equation (2).

1.1 An Hamiltonian formalism to relate the extension vs force function to the linear elasticity density.

We are now going to write the discretized form of the partition function given in equation (2) in terms of the transfer matrix operator \hat{T}_0 :

$$\begin{aligned} Z_0(\vec{r}_N, \vec{r}_0) &= \langle \vec{r}_N | \hat{T}_0^N | \vec{r}_0 \rangle, \\ \langle \vec{r}_{n+1} | \hat{T}_0 | \vec{r}_n \rangle &= \exp - \left(\epsilon_0 \left((\vec{r}_{n+1} - \vec{r}_n)^2 \right) - \vec{F} \cdot (\vec{r}_{n+1} - \vec{r}_n) \right). \end{aligned} \quad (3)$$

The operator \hat{T}_0 is invariant upon space translations and is then expected to be diagonal within the plane wave basis: $\langle \vec{r} | \vec{p} \rangle = (2\pi)^{-\frac{3}{2}} \exp(i\vec{p} \cdot \vec{r})$. The transfer matrix in the momentum space is then readily obtained :

$$\langle \vec{p}_{n+1} | \hat{T}_0 | \vec{p}_n \rangle = \delta^3(\vec{p}_{n+1} - \vec{p}_n) \tau_0 \left((\vec{p}_n - i\vec{F})^2 \right), \quad (4)$$

where $\tau_0(\vec{p}^2)$ is given in terms of $\epsilon_0(\vec{r}^2)$ by the following Fourier integral:

$$\tau_0(\vec{p}^2) = \int d^3 r \exp i\vec{p} \cdot \vec{r} \exp \left(-\epsilon_0(\vec{r}^2) \right). \quad (5)$$

Introducing the momentum operator $\hat{\vec{p}} = -i\vec{\nabla}$ the transfer matrix operator can be written under the simple form: $\hat{T}_0 = \tau_0 \left((\hat{\vec{p}} - i\vec{F})^2 \right)$. We arrive in this way to a compact formula for the partition function, which will lead us to the Hamiltonian \hat{H}_0 of an associated quantum mechanical problem:

$$\begin{aligned} Z_0(\vec{r}_N - \vec{r}_0, \vec{F}, N) &= \langle \vec{r}_N | \tau_0^N \left((\hat{\vec{p}} - i\vec{F})^2 \right) | \vec{r}_0 \rangle = \langle \vec{r}_N | \exp(-N\hat{H}_0) | \vec{r}_0 \rangle, \\ \hat{H}_0 &= h_0 \left((\hat{\vec{p}} - i\vec{F})^2 \right) = -\log \tau_0 \left((\hat{\vec{p}} - i\vec{F})^2 \right), \end{aligned} \quad (6)$$

where in our writing of the partition function we have made explicit the fact that Z_0 is invariant under space translation. In the simple case of the Gaussian model, one finds: $\hat{H}_0 = -\frac{b^2}{2} (\vec{\nabla} + \vec{F})^2$.

Let us proceed to the evaluation of the relative extension vs force function $\zeta_0(F)$. The extension average $\langle \vec{r} \rangle$ is given by :

$$\langle \vec{r} \rangle = \frac{\partial}{\partial \vec{F}} \log \left(\int d r^3 Z_0(\vec{r}, \vec{F}, N) \right) = -N \frac{\partial}{\partial \vec{F}} h_0(-\vec{F}^2). \quad (7)$$

Taking the stretching force along the z axis, one gets the relation which will allow us to construct the effective Hamiltonian \hat{H}_0 from the extension vs force curve $\zeta_0(f)$:

$$\zeta_0(F) = \frac{\langle z \rangle}{N} = 2F h'_0(-F^2) = -2f \frac{\tau'_0(-F^2)}{\tau_0(-F^2)}. \quad (8)$$

Let us now consider the case of the freely joining chain (FJC) which could be considered as a reasonable starting point for the study of self-avoiding effects for a "locally flexible" polymer. The transfer matrix operator for a chain of freely joining monomers, having a fixed length b , can be written as: $\langle \vec{r}_{n+1} | \hat{T}_0(FJC) | \vec{r}_n \rangle = \delta(|\vec{r}_{n+1} - \vec{r}_n| - b) \exp \vec{F} \cdot \vec{r}$. It can be easily written in momentum space form as in eq. (4) by taking: $\tau_0(\vec{p}^2) = \sin(pb)/(pb)$. Inserting this result in eq. (8), one gets immediately the FJC model extension vs force curve in terms of the reduced force $f = Fb$:

$$\zeta_{FJC}(f) = b \left(\coth(f) - \frac{1}{f} \right) = \frac{f}{3} - \frac{f^3}{45} + O(f^5). \quad (9)$$

1.2 Construction of an effective regular Hamiltonian from the extension vs force function.

If one applies blindly the formula (6) in order to get the effective Hamiltonian \hat{H}_0 , one gets $h_0(p^2) = -\log(\frac{\sin pb}{pb})$, which is clearly singular when $pb = n\pi$, n being an arbitrary non zero integer. One may try to regularize the model by replacing in $\langle \vec{r}_{n+1} | \hat{T}_0(FJC) | \vec{r}_n \rangle$ the δ function by a Gaussian, allowing for fluctuations of the monomer length b . This does not solve really the problem since $\tau_0(p^2)$ still oscillates around zero and $h_0(p^2)$ does not increase fast enough with p^2 . The fact that the above formal derivation of $h_0(p^2)$ leads to a singular result should not be considered as a surprise. A typical raw FJC contour line, in absence of any coarse-graining, is very far from what could be obtained by the discretization of a 3D-curve with smoothly varying derivatives of the running coordinate $\frac{d\vec{r}}{n}$.

We have adopted here the view that there is nothing sacred about the FJC model: it is just a guide to get a reasonable extension vs force curve for a "locally flexible" polymer.

Let us sketch the construction of a regular Hamiltonian $h_0^r(p^2)$ associated with an extension vs force function $\zeta_r(f)$ differing from $\zeta_{FJC}(f)$ by less than few % for

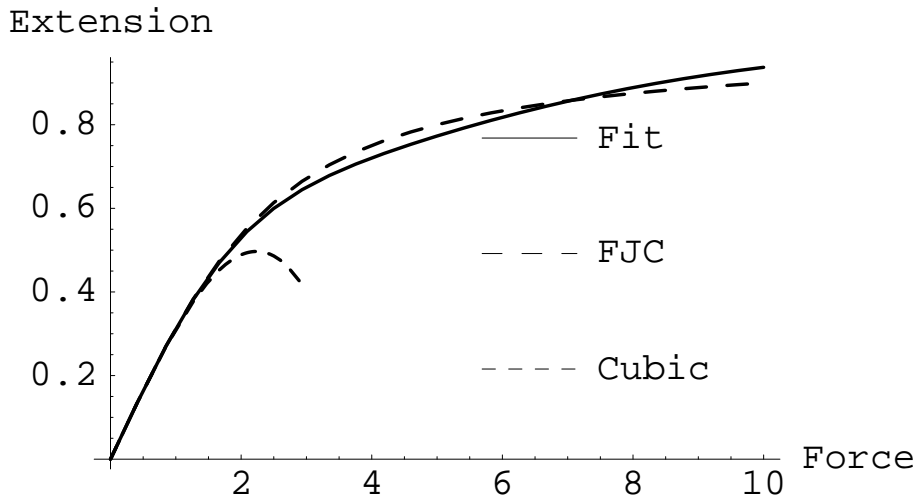


Figure 1: This figure gives the results of a fit of the extension vs force function $\zeta_{FJC}(f)$ by a superposition of two error functions. The idea behind this procedure is to build a continuous variant of the FJC mode, where the associated free Hamiltonian is regularized, while keeping the essential features of the FJC model elasticity. We see clearly on this figure that this goal has been successfully achieved. We have required the fitted function $\zeta_r(f)$, with the label "Fit" to coincide with $\zeta_{FJC}(f)$ to third order in the reduced force $f = F/b$. The dotted curve, with the label "Cubic", represents the third order polynomial expansion of $\zeta_{FJC}(f)$.

the whole range of values of the reduced force f . The result is exhibited on Fig.1. A convenient starting point is the derivative $\zeta'_{FJC}(f) = -\sinh^{-2}(f) + f^{-2}$. It is a bell-shaped even function of f we write as $\chi(f^2)$. In the case of the FJC model $\chi(z)$ is an analytic function of z with an infinite set of poles at $z_n = -(n\pi)^2$, which are responsible for the singularities of $h_0(p^2)$. We shall suppress them by replacing $\chi_{FJC}(z)$ by a function regular along the whole z , having the general form: $\chi_r(z) = \int_0^M dm g(m) \exp(-mz)$. Here $g(m)$ is a distribution which is non zero if and only if the real number m belongs to the finite domain $0 \leq m \leq M$ where M is a *finite positive real*. Note that this representation is not valid for $\chi_{FJC}(z)$ unless M is infinite.

As in all regularization methods, there is always some arbitrariness. Two criterion's have to be used as guiding principles: one is mathematical simplicity, the second is keeping to a minimum the number of *ad hoc* parameters. We have found that a very simple form of the distribution $g(m)$ is adequate for our purpose: $\chi_r(z)$ is taken as the sum of two exponentials. Returning to the f variable, it implies that the regularized bell-shaped curve $\zeta'(f)$ is the sum of two Gaussian. The main effect of the regularization is to change the shape of the high force tail of $\zeta'(f)$ in a domain where self-avoiding effects are becoming very weak. One of the peculiar feature of the analytic continuation $f \rightarrow ip$ is that a modification performed for large positive f values can induce or suppress singularities for finite values of $p : \pi, 2\pi \dots$.

By performing a simple quadrature, we arrive finally at the following expression for the regularized extension function $\zeta_r(f)$:

$$\zeta_r(f) = \frac{b}{2} ((1 - c) \operatorname{erf}(a_1 f) + (1 + c) \operatorname{erf}(a_2 f)), \quad (10)$$

where $\operatorname{erf}(z) = \frac{2}{\sqrt{\pi}} \int_0^\infty dt \exp -t^2$. Note that if a_1 and a_2 are positive, then $\zeta_r(\infty) = 1$. The determination of the parameters a_1 , a_2 and c is performed in two steps:

Step 1. a_1 and a_2 are obtained as functions of c by requiring the equality of the third order expansions of $\zeta_r(f)$ and $\zeta_{FJC}(f)$ with respect to f . As it is clear from Fig.1, this constraint insures that $\zeta_r(f)$ and $\zeta_{FJC}(f)$ coincide in the low to medium force range $0 \leq f \leq 1.5$, where self-avoiding effects are expected to be important.

Step 2. The parameter c results from a minimization of the mean square average difference : $\Delta_2(f_m) = \frac{1}{f_m} \int_0^{f_m} df (\zeta_r(f) - \zeta_{FJC}(f))^2$. For $|f| \geq 10$ the molecule extension is above 90% of its maximum. Self-avoiding effects are thus expected to be small, and this is confirmed by a look at the curves displayed on FIG. 7. This justifies our choice: $f_m = 10$. The resulting numerical values for the constrained parameters are then given by :

$$c = -0.035, \quad a_1 = 0.093, \quad a_2 = 0.484 \quad (11)$$

With the above numbers, one gets for the root mean square difference : $\sqrt{\Delta_2(f_m)} = 0.0198$. Such a small difference gives a measure of the success of our enterprise to suppress the singularities of $h_0(p^2)$ while keeping to a few percent level the modifications of the FJC model extension vs force function. It is also important to note that there is *no free parameter left*.

We are now ready to write down the effective Hamiltonian \hat{H}_0^r which will be used in this work :

$$\begin{aligned} \hat{H}_0^r &= h_0^r \left((\hat{p} - i\vec{F})^2 \right), \\ h_0^r(p^2) &= - \int_0^{pb} du \zeta_r(iu) \\ &= \frac{1}{2}(1 - c) \left(\frac{a_1}{\sqrt{\pi}} (1 - \exp(a_1 p^2 b^2)) + pb \operatorname{erfi}(a_1 p b) \right) \\ &\quad + (c \rightarrow -c, a_1 \rightarrow a_2), \end{aligned} \quad (12)$$

where $\operatorname{erfi}(z) = \operatorname{erf}(iz)/i$. The function $h_0^r(p^2)$ is displayed on Fig.2.

We have verified that the use of $h_0^r(p^2)$ does not introduce any significant non-physical artefact in the model. To do that, we have worked backward: taking $h_0^r(p^2)$ as starting point, we have computed the probability distribution of $l_n = |\vec{r}_{n+1} - \vec{r}_n|$, given by $\mathcal{P}(l_n) = l_n^2 \tilde{\tau}(l_n) = l_n^2 \exp -\epsilon_0(l_n^2)$. Using eq.(5), we get $\tilde{\tau}(l_n)$ by performing the 3D inverse Fourier transform of $\exp -h_0^r(p^2)$. Discarding a very weak damped

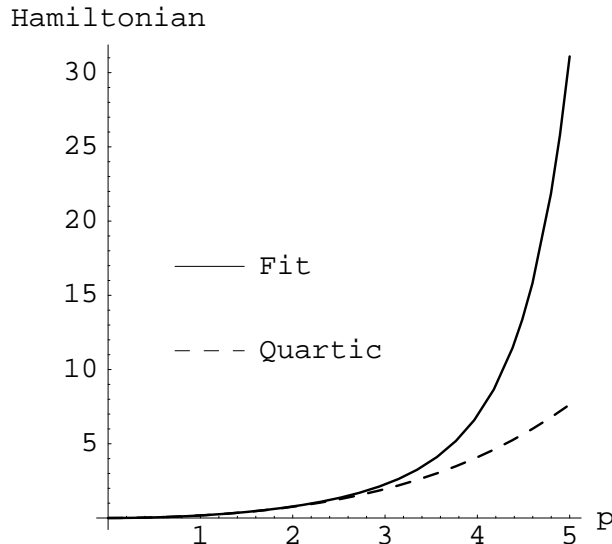


Figure 2: On this figure, the solid line represents the effective Hamiltonian $h_0^r(p^2)$, obtained by a simple quadrature from the analytic continuation $f \rightarrow ip$ of the force -extension curve $\zeta_r(f)$. The dashed curve gives the fourth order expansion: $h_0^{(4)}(p^2) = \frac{b^2 p^2}{6} + \frac{b^2 p^4}{180}$. It nearly coincides with $h_0^r(p^2)$ in the interval $0 \leq p \leq 3$ and will be used to get the analytic results given in this paper. Note the fast increase of two the curves for large values of p^2 . It guarantees the absence of divergences in the field theory description of self-avoiding effects which will be adopted in the present work.

oscillating tail at large l_n , having a maximum amplitude which stays below the 1.5% level, we get a well behaved Gaussian-like bell-shaped curve centered at $l_n \approx b$ with a half-width $\Delta l_n \approx b/2$. In our procedure, regularity conditions are enforced at each step. Our derived probability distribution $\mathcal{P}(l_n)$ is not expected to be a Dirac δ function but should rather be a peaked curve with a finite width, which should be of the order of the coarse-graining length resolution needed to wash out the strong fluctuations of the raw FJC contour line.

The quartic expansion of $h_0^r(p^2)$ is, by construction, independent of the parameters a_1, a_2 and c :

$$h_0^{(4)}(p^2) = \frac{b^2 p^2}{6} + \frac{b^2 p^4}{180} \quad (13)$$

As it is apparent on Fig 1 and 2, it could constitute an adequate starting point for the study of the self-avoiding effects of the FJC model in the force range $0 \leq f \leq 1.5$, which will be studied in the next sections. The effective Hamiltonian $\hat{H}_0^{(4)}$ associated with $h_0^{(4)}(p^2)$ can be viewed as a cutoff version of the Gaussian model. Indeed, the corresponding Green function in the momentum space: $\tilde{G}_0(p^2, z) = (z - h_0^{(4)}(p^2))^{-1}$ behaves as p^{-4} when $p^2 \gg \Lambda^2 = 30 b^{-2}$. The cut-off Λ is not here an *ad hoc* ingredient, since it is related to a simple physical quantity: the curvature of the extension vs force

curve in the low force regime.

We would like to stress that $h_0^{(4)}(-f^2)$ is not valid beyond $f \geq 2$. Higher polynomial expansion of $h_0(p^2) = -\log(\sin(p)/p)$, as a substitute for $h_0^r(p^2)$, will lead to difficulties due to the divergence of the entire series expansion of $h_0(p^2)$ at $p = \pi, 2\pi\dots$

2 The Hartree-Fock approximation for Self-avoiding Polymers.

Let us incorporate in the partition function the self-avoiding effects induced by the monomer-monomer repulsive central potential $g^2 V(|\vec{r}_1 - \vec{r}_2|)$:

$$Z(\vec{r}_N - \vec{r}_0, \vec{F}, N) = \int \mathcal{D}[\vec{r}] \exp - \int_0^N dn \left(\mathcal{E}_0(n) + \int_0^n dn' g^2 V(|\vec{r}_n - \vec{r}_{n'}|) \right). \quad (14)$$

Before entering into the details of our approximation scheme, it useful to derive a convenient formula for the evaluation of the chain extension vs force. We introduce the space average partition function $\bar{Z}(\vec{F}^2, N)$ obtained by integrating upon the distance $\vec{r} = \vec{r}_N - \vec{r}_0$ between the two free ends of the molecular chain.:

$$\bar{Z}(\vec{F}^2, N) = \int d r^3 Z(\vec{r}, \vec{F}, N) = \int d r^3 \exp(\vec{r} \cdot \vec{F}) Z(\vec{r}, 0, N), \quad (15)$$

where we have factorized the stretching potential energy and exploited the rotation invariance of $Z(\vec{r}, 0, N)$. Taking the stretching force along the z axis, $\vec{F} = \hat{z} F$, we can readily obtain the relative extension vs force expression :

$$\zeta(F, N) = \frac{\langle z \rangle}{N} = \frac{\partial}{N \partial F} \log \left(\bar{Z}(F^2, N) \right). \quad (16)$$

The computation method developed in this section will give in a rather direct way the Fourier transform of the partition function of the unstretched polymer:

$$\tilde{Z}(k^2, N) = \int d r^3 \exp(i \vec{r} \cdot \vec{k}) Z(\vec{r}, 0, N). \quad (17)$$

It is then of interest to write the extension vs force formula in terms of this quantity. To do that, let us take again \vec{F} along the z axis and perform the analytic continuation $F \rightarrow ip$ upon the r.h.s. of eq. (15). Inserting the Fourier expansion of $Z(\vec{r}, 0, N)$, one can readily integrate over \vec{r} and arrive at the relation $\tilde{Z}(p^2, N) = \bar{Z}(-p^2, N)$. Performing the analytic continuation backwards, one gets the searched-for formula:

$$\zeta(F, N) = \frac{\langle z \rangle}{N} = \frac{\partial}{N \partial F} \log \left(\tilde{Z}(-F^2, N) \right). \quad (18)$$

2.1 *A Statistical Field Theory model for self-avoiding effects in flexible polymers .*

Following a standard procedure [13, 14], we are going to transform the evaluation of the r.h.s. of (14) into a field theory problem involving an auxiliary scalar field $\phi(\vec{r})$. The basic tool is the well known Gaussian functional integral identity :

$$\begin{aligned} \mathcal{E}[V] &= \exp -\frac{1}{2} \int_0^N dn \int_0^N dn' g^2 V(|\vec{r}_n - \vec{r}_{n'}|) & (19) \\ &= (\det V)^{1/2} \int \mathcal{D}[\phi] \exp - \left(\int_0^N dn i g \phi(\vec{r}_n) \right) \\ &\quad \times \exp - \left(\int d^3 r_1 d^3 r_2 \frac{1}{2} V^{-1}(\vec{r}_1 - \vec{r}_2) \phi(\vec{r}_1) \phi(\vec{r}_2) \right). & (20) \end{aligned}$$

In the case of the Yukawa potential $V(r) = \frac{1}{4\pi r} \exp -r/a$, the inverse operator is given by :

$$V^{-1}(\vec{r}_1 - \vec{r}_2) = \delta^3(\vec{r}_1 - \vec{r}_2) (-\vec{\nabla}_1^2 + a^{-2}).$$

We arrive in this way to the Field Theory formula for the partition function upon which we are going to build our approximation scheme:

$$\begin{aligned} Z(\vec{r}_N - \vec{r}_0, \vec{F}, N) &= \int \mathcal{D}[\phi] \exp - \left(\int d^3 r_1 d^3 r_2 \frac{1}{2} V^{-1}(\vec{r}_1 - \vec{r}_2) \phi(\vec{r}_1) \phi(\vec{r}_2) \right) \\ &\quad \times \langle \vec{r}_N | \exp -N \hat{H}(\vec{F}, \phi) | \vec{r}_0 \rangle. & (21) \end{aligned}$$

The Hamiltonian $\hat{H}(\vec{F}, \phi)$ involves the stochastic imaginary potential $i g \phi(\vec{r})$:

$$\hat{H}(\vec{F}, \phi) = h_0 \left((\hat{p} - i\vec{F})^2 \right) + i g \phi(\vec{r}), \quad (22)$$

where the "kinetic" term $h_0(p^2)$ is to be identified with $h_0^{(4)}(p^2)$ (eq. (13)), or eventually with $h_0^r(p^2)$ (eq. (12)).

2.2 *A simple Feynman graph expansion for the Laplace transform of the partition function.*

We proceed by performing the Laplace transform of (21) with respect to N :

$$\begin{aligned} z(\vec{r}_N - \vec{r}_0, \vec{F}, \tau) &= \int_0^\infty dN \exp(-\tau N) Z(\vec{r}_N - \vec{r}_0, \vec{F}, N) \\ &= \langle \vec{r}_N | \langle (h_0 \left((\hat{p} - i\vec{F})^2 \right) + i g \phi(\vec{r}) + \tau)^{-1} \rangle_\phi | \vec{r}_0 \rangle, & (23) \end{aligned}$$

where we have introduced a compact notation to describe the average of a given functional $\mathcal{F}[\phi]$ over the stochastic field $\phi(\vec{r})$:

$$\langle \mathcal{F}[\phi] \rangle_\phi = \int \mathcal{D}[\phi] \mathcal{F}[\phi] \exp - \left(\int d^3 r_1 d^3 r_2 \frac{1}{2} V^{-1}(\vec{r}_1 - \vec{r}_2) \phi(\vec{r}_1) \phi(\vec{r}_2) \right). \quad (24)$$

One sees immediately that the average product of an odd number of fields $\phi(\vec{r}_i)$ is zero. We give some simple examples of even products:

$$\begin{aligned} \langle \phi(\vec{r}_1) \phi(\vec{r}_1) \rangle_0 &= V(|\vec{r}_1 - \vec{r}_2|) \\ \langle \phi(\vec{r}_1) \phi(\vec{r}_2) \phi(\vec{r}_3) \phi(\vec{r}_4) \rangle_0 &= V(|\vec{r}_1 - \vec{r}_2|) V(|\vec{r}_2 - \vec{r}_4|) + V(|\vec{r}_1 - \vec{r}_4|) V(|\vec{r}_2 - \vec{r}_3|) \\ &\quad + V(|\vec{r}_1 - \vec{r}_3|) V(|\vec{r}_2 - \vec{r}_4|) \end{aligned} \quad (25)$$

The rule is easily generalized to a product of an arbitrary even number of fields and leads readily to a Feynman graph expansion of $z(\vec{r}, \vec{F}, \tau)$ in power of g^2 . The perturbation expansion of the resolvent $R(\tau) = (\hat{H}_0 + \hat{U} + \tau)^{-1}$ (the operator \hat{U} is defined by $\langle \vec{r}_2 | \hat{U} | \vec{r}_1 \rangle = i g \delta^3(\vec{r}_1 - \vec{r}_2) \phi(\vec{r}_1)$) is given by the geometrical series, keeping only the relevant even terms :

$$\begin{aligned} R(\tau) &= R_0(\tau) + R_0(\tau) \hat{U} R_0(\tau) \hat{U} R_0(\tau) \\ &\quad + R_0(\tau) \hat{U} R_0(\tau) \hat{U} R_0(\tau) \hat{U} R_0(\tau) \hat{U} R_0(\tau) + \dots, \end{aligned} \quad (26)$$

where $R_0(\tau) = (\hat{H}_0 + \tau)^{-1}$. To make more apparent the analogy with the Field Theory formalism we define the Green functions:

$$\begin{aligned} G_0(\vec{r}_2 - \vec{r}_1, \tau) &= z_0(\vec{r}_2 - \vec{r}_1, \vec{F}, \tau) = \langle \vec{r}_2 | R_0(\tau) | \vec{r}_1 \rangle \\ G(\vec{r}_2 - \vec{r}_1, \tau) &= z(\vec{r}_2 - \vec{r}_1, \vec{F}, \tau) = \langle \vec{r}_2 | \langle R(\tau) \rangle_\phi | \vec{r}_1 \rangle \end{aligned} \quad (27)$$

2.3 An Hartree-Fock approximation from the Dyson equation.

Following Dyson [15], we introduce the proper self-energy $\Sigma(\vec{r}_2 - \vec{r}_1)$ obtained by summing all self-energy diagrams which cannot be divided into two disconnected pieces by cutting the "particle line" associated with the Green functions $G_0(\vec{r}_2 - \vec{r}_1, \tau)$. Pure topological arguments lead to the well known Dyson equation for the propagator:

$$\begin{aligned} G(\vec{r}_2 - \vec{r}_1, \tau) &= G_0(\vec{r}_2 - \vec{r}_1, \tau) + \\ &\quad \int d^3r_3 d^3r_4 G_0(\vec{r}_2 - \vec{r}_3, \tau) \Sigma(\vec{r}_3 - \vec{r}_4) G(\vec{r}_4 - \vec{r}_1, \tau). \end{aligned} \quad (28)$$

Taken in their exact form, the Dyson equations have played a very important role in the Renormalization Theory but they are of little use for practical computations. They are, however, very convenient to devise non trivial infinite summation scheme by taking an approximate form of the proper self-energy. The best known example of this procedure is the Hartree-Fock (HF) method ² which relies upon the approximate formula:

$$\Sigma(\vec{r}_2 - \vec{r}_1) \approx \Sigma^{(1)}(\vec{r}_2 - \vec{r}_1) = -g^2 G(\vec{r}_2 - \vec{r}_1, \tau) V(\vec{r}_2 - \vec{r}_1) \quad (29)$$

² The formalism used here takes its inspiration from the Fetter and Walecka remarkable book dealing, with Quantum Theory of Many Particle Systems [12].

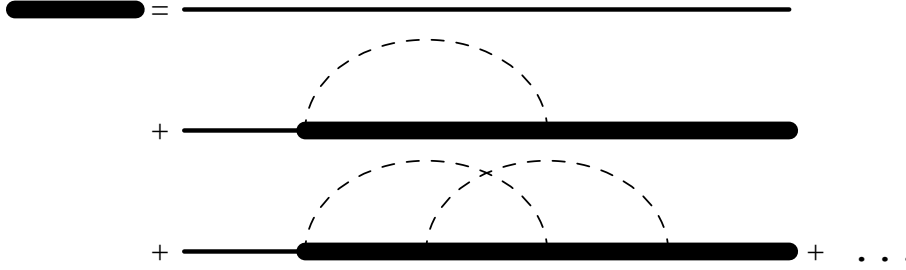


Figure 3: Graphical representation of the Hartree-Fock approximation. The thin line and the thick lines stand respectively for the free and the self-avoiding polymer Green functions. The dashed half-ellipses represent the self-avoiding interactions. The two upper diagrams schematize the HF approximation used in this paper which performs the summation of the planar graphs. An infinite set of non-planar diagrams is generated by including the contribution of the bottom diagram.

A physical interpretation of the HF approximation can be given by noting that $\Sigma^{(1)}(\vec{r}_2 - \vec{r}_1)$ is obtained by replacing, in the lowest order proper self-energy, the free polymer propagator $G_0(\vec{r}, \tau)$ by $G(\vec{r}, \tau)$ which incorporates in a self consistent way higher order monomer-monomer interactions. Although technically rather different, the present HF method bears a close analogy to the "rainbow" diagrams summation method used to compute "hairpin" effects in a single stranded discretized DNA chain[11].

One of the virtues of the Field Theory formulation of the Hartree-Fock method is to allow a rather systematic treatment of the correcting terms. The first step consists in adding to the HF proper self-energy given by eq.(29) a correction term $\Sigma^{(2)}(\vec{r}_2 - \vec{r}_1)$ which will generate an infinite set of non-planar diagrams. It is constructed from the lowest order *non-planar* diagram contribution to the proper self-energy in the same way as $\Sigma_{HF}(\vec{r}_2 - \vec{r}_1)$ was obtained from the lowest order proper self energy:

$$\Sigma^{(2)}(\vec{r}_2 - \vec{r}_1) = g^4 \int d^3r_3 d^3r_4 G(\vec{r}_2 - \vec{r}_4) V(\vec{r}_2 - \vec{r}_3) \times G(\vec{r}_4 - \vec{r}_3) V(\vec{r}_4 - \vec{r}_1) G(\vec{r}_3 - \vec{r}_1). \quad (30)$$

We give in FIG.3 a graphical representation of the H.F procedure. The thin lines stand for free polymer Green function $G_0(\vec{r}, \tau)$, while the thick ones correspond to the self-avoiding polymer Green function $G(\vec{r}, \tau)$. The calculations performed in the present paper incorporate the contribution of the two upper diagrams. The correction associated with $\Sigma^{(2)}(\vec{r}_2 - \vec{r}_1)$ will be very briefly discussed in the next section.

2.4 The HF equation in momentum space.

Because of the space translation invariance of eq. (28) considerable simplification is achieved by working within the plane wave basis where the operators \hat{G}, \hat{G}_0 and $\hat{\Sigma}$

are diagonal :

$$\begin{aligned}\langle \vec{p}_2 | \hat{G} | \vec{p}_1 \rangle &= \langle \vec{p}_2 | \langle R(\tau) \rangle_\phi | \vec{p}_1 \rangle = \delta^3(\vec{p}_1 - \vec{p}_2) \tilde{G}(\vec{p}_1, \tau) \\ &= \delta^3(\vec{p}_1 - \vec{p}_2) \int d^3 r \exp(i \vec{p}_1 \cdot \vec{r}) G(\vec{r}).\end{aligned}\quad (31)$$

The Hartree-Fock integral equation can then be written under the rather compact form:

$$\begin{aligned}\tilde{G}(\vec{p}_1, \tau)^{-1} &= \tilde{G}_0(\vec{p}_1, \tau)^{-1} - \tilde{\Sigma}(\vec{p}_1, \tau) \\ &= \tilde{G}_0(\vec{p}_1, \tau)^{-1} + \frac{g^2}{(2\pi^3)} \int d^3 p \tilde{G}(\vec{p}, \tau) \tilde{V}(|\vec{p}_1 - \vec{p}|).\end{aligned}\quad (32)$$

In order to compute the extension vs force curve in the general case, one has to proceed as follows:

i) First, we take the limit $\vec{F} = 0$. The operators $R_0(\tau)$ and $\langle R(\tau) \rangle_\phi$ are then rotation invariant and $\tilde{G}(\vec{p}, \tau) = \tilde{g}(p^2, \tau)$. The HF integral equation becomes one-dimensional with as kernel $K(p_1, p) = 2\pi p^2 \int_{-1}^1 dx \tilde{V}(\sqrt{p_1^2 - p^2 - 2xp_1p})$. In the particular case of Yukawa or exponential potentials, $K(p_1, p)$ is easily computed analytically. Returning to Statistical Mechanics notations one sees on eq.(27) that $\tilde{g}(p^2, \tau)$ is nothing but the Laplace transform $\tilde{z}(p^2, \tau)$ of $\tilde{Z}(p^2, N)$, introduced in eq.(17).

ii) The second step involves the analytic continuation $p^2 \rightarrow -F^2$ of $\tilde{z}(p^2, \tau)$. Then, one has to perform the inverse Laplace transform in order to get the extension vs force curve $\zeta(F, N)$ from eq.(18). As we shall see, for the particular case of the δ function potential, $\zeta(F, N)$ is dominated in the large N limit by the contribution of the pole of $\tilde{g}(-F^2, \tau) = \tilde{z}(-F^2, \tau)$, occurring at the largest algebraic value of τ .

3 The HF Method for a Short Range Repulsive Monomer-Monomer Potential.

From now on, we are going to use b as the unit of length and as before $k_B T$ as the unit of energy. The short range limit of the Yukawa potential $g^2 V(r) = \frac{g^2 a}{4\pi r} \exp -\frac{r}{a}$, is obtained by taking $a \rightarrow 0$, keeping $g^2 a^3$ finite. The result is just the δ -function potential : $V(\vec{r}) = g^2 a^3 \delta^3(\vec{r})$. The HF proper self-energy reduces to: $\Sigma(\vec{r}_2 - \vec{r}_1) = -g^2 a^3 G(0, \tau) \delta^3(\vec{r}_2 - \vec{r}_1)$. This implies: $\tilde{\Sigma}(\vec{p}, \tau) = -g^2 a^3 G(0, \tau)$.

3.1 The reduction of the HF integral equation to a numerical equation.

The Green function in momentum space is then given by :

$$\tilde{G}(\vec{p}, \tau) = \tilde{g}(p^2, \tau) = \left(h_0(p^2) + \tau + g^2 a^3 G(0, \tau) \right)^{-1}.\quad (33)$$

By computing $G(\vec{r}, \tau)$ from the above equation by a Fourier integral and then taking the limit $\vec{r} \rightarrow 0$, one gets a self-consistent equation giving $G(0, \tau)$:

$$G(0, \tau) = \frac{1}{2\pi^2} \int_0^\infty \frac{p^2 dp}{h_0(p^2) + \tau + g^2 a^3 G(0, \tau)} . \quad (34)$$

From now on, we shall take $h_0(p^2) = h^{(4)}(p^2) = \frac{1}{6} p^2 + \frac{1}{180} p^4$. (Remember that our length unit is b). With our choice of $h_0(p^2)$ the integral in the r.h.s. is clearly convergent, while it would have been linearly divergent in the case of the free Gaussian chain. We have found convenient to use instead of $G(0, \tau)$ the following self-consistent function:

$$\mu(\tau) = \tau + g^2 a^3 G(0, \tau). \quad (35)$$

To solve exactly the HF equation we have introduced the algebraic function :

$$F(\kappa, \tau) = \int_0^\infty \frac{p^2}{p^2 + p^4 \kappa^2 + \tau} = \frac{\pi \left(-1 + 2 \kappa \sqrt{\tau} + \sqrt{1 - 4 \kappa^2 \tau} \right)}{\sqrt{2 \kappa} \sqrt{1 - 4 \kappa^2 \tau} \sqrt{1 - \sqrt{1 - 4 \kappa^2 \tau}}}, \quad (36)$$

where we have made explicit for clarity the cutoff parameter $\kappa^2 = b^2/\Lambda^2 = 1/30$. In order to study the cross-over occurring in the vicinity of $f = 0$, the following approximation of $F(\kappa, \tau)$ is useful:

$$F_0(\kappa, \tau) = \frac{\pi}{2 \kappa} \left(1 - \kappa \sqrt{\tau} + \frac{3 \kappa^2 \tau}{2} + O(\kappa \sqrt{\tau})^3 \right). \quad (37)$$

We are now ready to write down the self-consistent equation giving $\mu(\tau)$:

$$\begin{aligned} \mu(\tau) &= \tau + \frac{\lambda}{6} F(\kappa, 6\mu(\tau)), \\ \lambda &= \frac{18}{\pi^2} g^2 a^3. \end{aligned} \quad (38)$$

Remembering that $\tilde{g}(-f^2, \tau) = \tilde{z}(-f^2, \tau) = (h_0(-f^2) + \mu(\tau))^{-1}$ is the Laplace transform the searched-for quantity $\tilde{Z}(-f^2, N)$, one has to perform the following inverse Laplace transform:

$$\tilde{Z}(-f^2, N) = \frac{1}{2 \pi i} \int_{\epsilon - i \infty}^{\epsilon + i \infty} d\tau \exp(N \tau) \left(h_0(-f^2) + \mu(\tau) \right)^{-1}.$$

It appears that the relevant singularities of $\tilde{g}(-f^2, \tau)$, in the complex half plane $\Im(\tau) < 0$, are lying along the negative real half axis. As a consequence, the integration contour along the imaginary τ axis can be folded around the negative real half axis. This leads to the following integral formula :

$$\tilde{Z}(-f^2, N) = \frac{1}{2 \pi i} \left(\int_{0+i\epsilon}^{-\infty+i\epsilon} + \int_{-\infty-i\epsilon}^{0-i\epsilon} \right) d\tau \exp(N \tau) \left(h_0(-f^2) + \mu(\tau) \right)^{-1}. \quad (39)$$

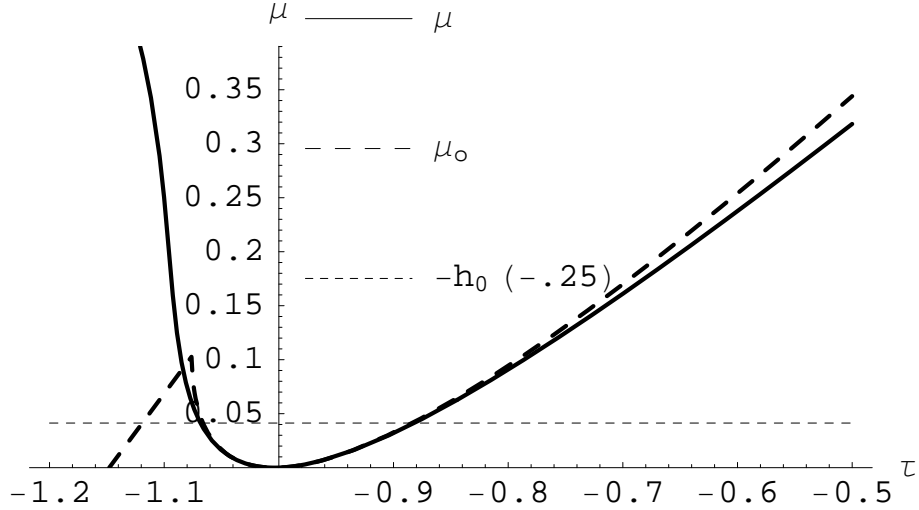


Figure 4: The partition function $\tilde{Z}(-f^2, N)$ is obtained from the inverse Laplace transform of $(h_0(-f^2) + \mu(\tau))^{-1}$. The result is dominated by the pole residues of the integral. Since $h_0(-f^2) \leq 0$, we have to look for the positive solutions of $\mu(\tau) = \tau + \frac{\lambda}{6}F(\kappa, 6\mu(\tau))$. The continuous line gives the self consistent function $\mu(\tau)$ for $\lambda = 0.7$. The dashed line is associated with the approximate function $\mu_0(\tau)$, obtained with the simplified function $F_0(\kappa, \tau)$, valid for small τ up to corrections of order $(\frac{\tau}{30})^{3/2}$. The figure shows that this approximation is adequate in the region below the horizontal dotted line, which corresponds to the low force interval $0 \leq f \leq 0.5$.

3.2 Analytical computations of the extension vs force curves in the low force regime.

Let us consider first the low force regime $0 \leq f \leq 0.5$ i.e $0 \leq -h_0(-f^2) \leq 0.0413$. We are clearly interested by the value of $\mu(\tau) \simeq -h_0(-f^2) \leq 0.0413$. The use of the approximation $F(\kappa, 6\mu(\tau)) \simeq F_0(\kappa, 6\mu(\tau))$ is justified here by the small value expansion parameter : $\kappa\sqrt{6\mu(\tau)} \leq 0.091$. The corresponding approximate function $\mu_0(\tau)$ differs from the exact one by less than 0.5% if $0 \leq f \leq 0.5$, as it is seen clearly

on FIG. 4. Let us look first for the value $\tau = \tau_c = \frac{-(\sqrt{\frac{5}{6}}\pi\lambda)}{2}$ such that $\mu(\tau_c) = 0$. It is convenient to define the translated variable $\sigma = \tau - \tau_c$. To get an explicit expression of $\mu_0(\tau)$, what we have done first is to solve the self-consistent equation for $\tau > 0$. In this region, $\mu_0(\tau) > 0$, so that the function $F_0(\kappa, 6\mu_0(\tau))$ is regular. We perform next an analytic continuation toward the point $\tau = \tau_c$ where $\mu_0(\tau)$ vanishes. According to eq. (refinvlap), we have to follow paths running just above (and below) the half negative half axis. This insures that $\sqrt{\mu^2} = \mu$ in the vicinity of $\tau = \tau_c$. We arrive then to the following explicit formula, valid in the region of physical interest:

$$\begin{aligned}
\mu_0(\tau_c + \sigma) &= \frac{240 \sigma^2}{240 \sigma + \pi \lambda \left(5 \pi \lambda - 6 \sqrt{30} \sigma + \sqrt{2400 \sigma + 5 \pi \lambda (5 \pi \lambda - 12 \sqrt{30} \sigma)} \right)} \\
&= \frac{24 \sigma^2}{\pi^2 \lambda^2} + \frac{144 (-40 + \sqrt{30} \pi \lambda) \sigma^3}{5 \pi^4 \lambda^4} + O(\sigma^4). \tag{40}
\end{aligned}$$

Some remarks are in order : first, the above expression has for small value of $\tau - \tau_c$, the parabolic shape exhibited on FIG.4, second a branch point occurs for $\tau - \tau_c = \tau_b = \frac{5 \pi^2 \lambda^2}{-480 + 12 \sqrt{30} \pi \lambda}$. It manifests its presence on the curves of FIG.4 by a spike. (Below the branch point it is actually $\Re(\mu_0(\tau))$ which is plotted.) Such a singularity does not seem to show up in the range of interest for the exact function $\mu(\tau)$ and it is likely to be an artefact of the approximation $F(\kappa, 6\mu(\tau)) \simeq F_0(\kappa, 6\mu(\tau))$. Nevertheless, we have computed explicitly its contribution to the inverse Laplace transform and it was found to be negligible compared to the dominant poles contributions. Finally it is of interest to note that the coefficient of the series expansions with respect to σ are divergent in the weak coupling limit $\lambda \rightarrow 0$. Furthermore, we have checked the identity of series expansion in power of λ obtained by two different ways: one, by a direct expansion of the above exact expression of $\mu_0(\tau)$, two, by solving the self-consistent equation by a perturbation method. The coefficients of the various powers of λ have a branch cut at $\tau = 0$ which disappear when the exact summation is performed. The above remarks provides an illustration, on a simple case, of the importance of non-perturbative effects in the self-avoiding polymers problem.

The two poles $\tau_{1,2}(f, \lambda)$ of $(h_0(-f^2) + \mu_0(\tau))^{-1}$ are easily computed:

$$\begin{aligned}
\tau_{1,2}(f, \lambda) &= \tau_c \pm \frac{\pi \eta(f) \lambda}{2 \sqrt{6}} + \eta(f)^2 \left(1 - \frac{\sqrt{\frac{3}{10}} \pi \lambda}{4} \right), \\
\eta(f) &= f \sqrt{1 - \frac{1}{30} f^2}. \tag{41}
\end{aligned}$$

We have in hands all the information needed to compute the partition function $\tilde{Z}(-f^2, N)$ given by eq. (39). Ignoring the branch point contribution, we are left with the residue contributions relative to the two poles at $\tau = \tau_{1,2}(f, \lambda)$:

$$\tilde{Z}(-f^2, N) = \sum_{i=1}^2 \exp(N \tau_i(f, \lambda)) \left(\frac{\partial \mu_0(\tau_i(f, \lambda))}{\partial \tau} \right)^{-1}. \tag{42}$$

The relative extension $\zeta(f, N) = \langle z(N) \rangle / N$ is then given by the logarithmic derivative:

$$\zeta(f, N) = -\frac{1}{N} \frac{\partial}{\partial f} \log \left(\tilde{Z}(-f^2, N) \right). \tag{43}$$

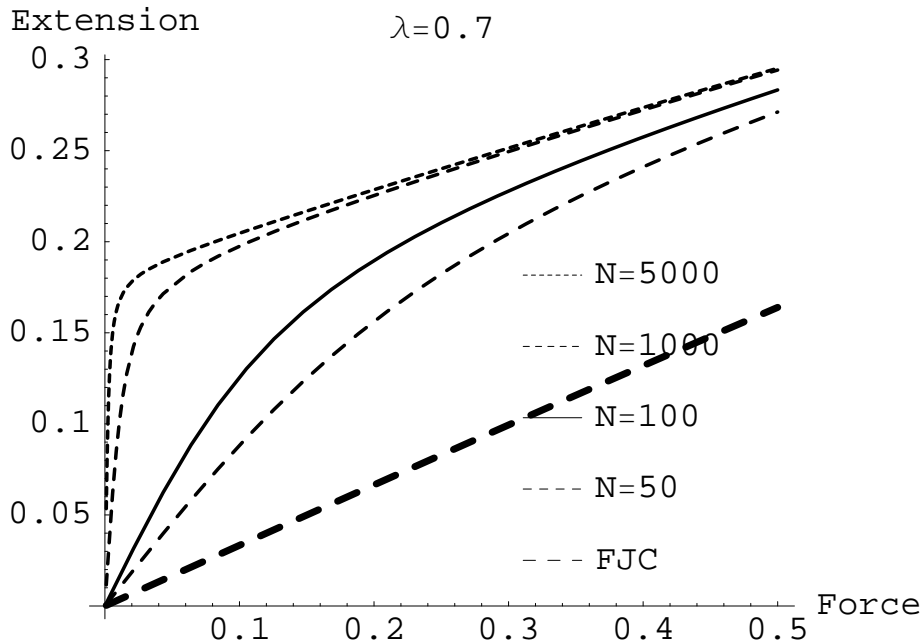


Figure 5: On this figure we have displayed a set of extension vs force curves in the low energy regime, for typical values of the monomer number N . The bottom thick dashed curve represents the FJC extension vs force curve with no self-avoidance. The most remarkable feature is the steady increase with N of the slopes at the origin ($f = 0$). We note also that in the limit of very large N , the extension jumps to a finite value at very small force. This suggests the presence of a cross-over phenomena near $f = 0$. This could be associated with the partition function Laplace transform poles crossing at the origin.

Using the explicit formulas for $\mu_0(\tau)$ and $\tau_i(f, \lambda)$ given in eq. (40) and (41), $\zeta(f, N)$ can be computed analytically. The corresponding expression is rather involved and not very illuminating. A better illustration of what is going on in the low force regime is obtained by looking at FIG.5 where relative extension vs force curves $\zeta(f, N) = \langle z(N) \rangle / N$ are displayed for increasing values of the total chain monomer number N .

3.3 Comparison of HF extension slopes at the origin ($f=0$) with the results derived from RG arguments.

The most salient feature of these curves lies in the fact that the extension vs force curve slope, $s(N, \lambda) = \left. \frac{\partial E(f, N)}{\partial f} \right|_{f=0}$, increases with N , while it stays constant in the case of the FJC model. This kind of behaviour is found under a less pronounced form in the Edwards model (Gaussian chain with short range self-avoidance), using renormalization group arguments (RG). We would like to stress that a quantitative

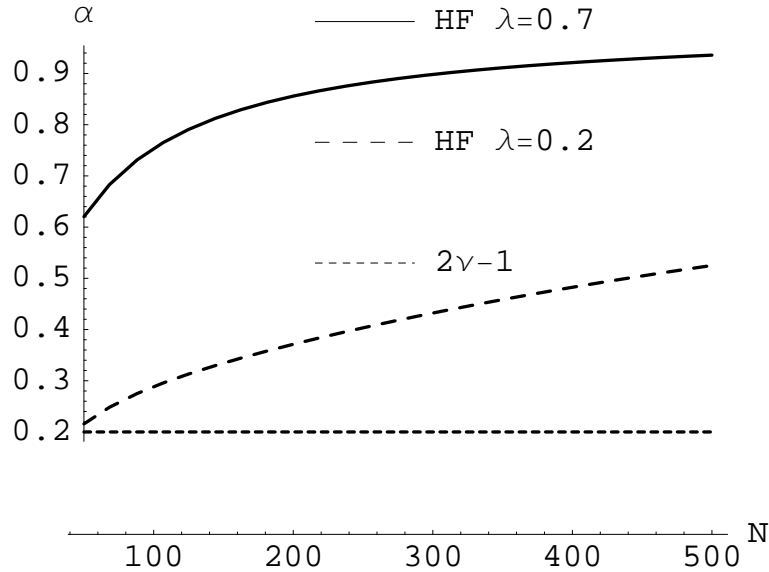


Figure 6: In this figure we present the results of a simple analysis of the variation of the slope of the extension vs force curve $s(N, \lambda)$ at $f = 0$ with the monomer number N . We have plotted the characteristic quantity $\alpha(N, \lambda)$ defined as N times the logarithmic derivative of the slope at the origin with respect to N . If $\alpha(N, \lambda)$ stays constant, the slope behave as N^α or, in other words, it obeys a scaling law. RG arguments applied to the Edwards model gives $\alpha = 2\nu - 1$, where $\nu \simeq 0.6$ is the Flory coefficient. Our model exhibits a moderate but significant variation of $\alpha(N, \lambda)$ with N . Moreover, $\alpha(N, \lambda)$ is not "universal", in the sense that it is roughly proportional to the coupling constant λ . We would like to stress that this difference was to be expected. As we have pointed out previously, our model can be viewed as a fixed cutoff ($\Lambda^2 = 30/b^2$) version of the Edwards model and, as a consequence, RG arguments are not valid.

comparison of the two approaches is not a simple problem. We have noted previously that the model used in the present paper can be viewed as a version of the Edwards model, endowed with a *fixed cutoff* $\Lambda^2 = \frac{30}{b^2}$. It is then clear that under such circumstances RG arguments are not appropriate.

For exhibiting the difference of behavior in the vicinity of $f = 0$, it is convenient to introduce the following quantity : $\alpha(N, \lambda) = N \frac{\partial}{\partial N} \log (s(N, \lambda))$. Its physical interpretation becomes more apparent by noting that if $\alpha(N, \lambda)$ is constant, then the slope $s(N, \lambda)$ is proportional to N^α . This corresponds to the scaling prediction [16] for the Edwards model with $\alpha = 2\nu - 1$, where $\nu \simeq \frac{3}{5}$ is the Flory coefficient, which governs the variation of the root mean square radius of the Edwards chain in absence of stretching force : $\sqrt{\langle r^2(N) \rangle} \propto N^\nu$. Curves giving the variation of $\alpha(N, \lambda)$ are displayed on FIG.6. In the case of the present HF computations, there is, for fixed λ , a moderate but significant increase of $\alpha(N, \lambda)$ with N . Moreover, for fixed N , when λ goes from 0.2 to 0.7, $\alpha(N, \lambda)$ is multiplied by a factor varying from 3 to 2 when N

increases from 50 to 500.

These features are likely to be associated with the fact that we are dealing with a fixed cutoff field theory problem but they could also be partly due to an artefact of the Hartree-Fock approximation. In order to check this latter point, one should try to estimate the corrections to the HF approximation. In the particular case of the short range repulsive potential $g^2V(\vec{r}) = a^3g^2\delta(\vec{r})$, the proper self-energy correction $\Sigma^{(2)}(\vec{r}_2 - \vec{r}_1)$ is given by the rather simple expression:

$$\Sigma^{(2)}(\vec{r}_2 - \vec{r}_1) = g^4a^6 (G(\vec{r}_2 - \vec{r}_1))^2 \quad (44)$$

The self-consistent integral equation cannot be reduced anymore to the solving of a numerical equation. The resulting non-linear integral equation can be solved by an iteration procedure starting from the HF approximation. Such a calculation, which looks feasible, is clearly of considerable interest but it falls outside the scope of the present exploratory paper.

4 Comparison of the Hartree-Fock Force vs Extension Curves Computations with the Results of Monte-Carlo Simulations

In this last section we would like to compare the results of the Hartree-Fock method applied to the self-avoiding effects for a continuous version of the FJC model with those obtained by a Monte-Carlo simulation of a self-avoiding freely joining chain.

We begin by saying some words about the way we have obtained the theoretical force vs extension curve displayed on FIG.7. In the range: $0 < f < 0.25$ we have used the analytic formulas of the previous section, which are valid in the low force regime. In the medium force interval : $0.2 < f < 1.5$ the computation was performed with the exact solution $\mu(\tau)$ of the self-consistent equation (38). A considerable simplification was achieved by noting that, if $f > 0.2$, the pole residue at $\tau = \tau_1(f, \lambda) > \tau_2(f, \lambda)$ gives the dominant contribution, by more than two orders of magnitude.

Above $f = 1.5$ we are leaving the domain of strict validity of our computation. We have performed an extrapolation to cover the interval $1.5 < f < 3.0$. It corresponds to the dashed part of the theoretical curve of FIG.7. We do not extrapolate directly the final result but rather the quantity $\tilde{g}(-f^2, \tau)^{-1} = h_0(-f^2) + \mu(\tau)$. For the first term, we set $h_0(-f^2) = h_0^r(-f^2)$, instead of keeping $h_0^4(-f^2)$ which would lead to an inadequate force vs extension curve for $f > 2$, as it appears clearly on FIG.1. Concerning $\mu(\tau)$, we note two things: first, the replacement $h_0^4(p^2) \rightarrow h_0^r(p^2)$ will only affect the high p tail of the convergent integral giving the function $F(\kappa, \tau)$ (see FIG.2), second, the non corrected $\mu(\tau)$ varies linearly in the interval of interest: $0.35 < \mu(\tau) < 1.2$. It look then reasonable to perform our extrapolation by keeping the self-consistent function $\mu(\tau)$ given by eq.(38).

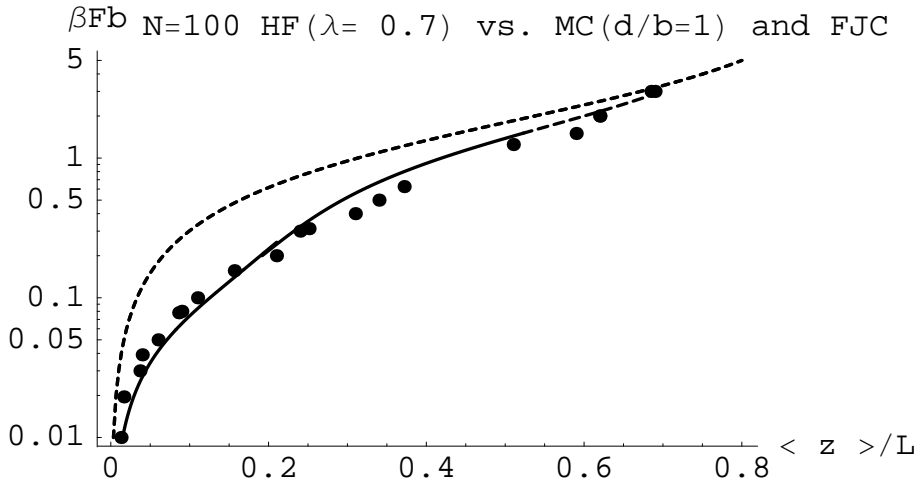


Figure 7: This figure presents a comparison of the force vs extension curves for $N = 100$ obtained, on one hand, from the HF analytic computations of the present paper, on the other hand, from MC simulations performed by the ENS experimental group. Our analytic treatment, represented by the continuous curve, is strictly valid in the low to medium force range $0 \leq f \leq 1.5$. Nevertheless, we have performed a reasonably safe extrapolation - the dotted branch of the curve- in order to cover the higher force range $1.5 \leq f \leq 3$. The choice of the value of our single parameter: $\lambda = 0.7$ does not come out from a least square fit but from a trial and error procedure. In the MC simulations self-avoidance was implemented by keeping only the configurations such that the distances between any two non -adjacent monomers are larger than a fixed length d . In the actual simulations b was taken equal to the fixed distance b between adjacent polymers. The fairly good agreement between these two different approaches is quite remarkable and it may suggest the shape of the force curves is not very sensitive to the range of the repulsive potential if $d \leq b$.

The M.C simulation results displayed as big dots on FIG.7 have been obtained by the authors of reference [10], with a chain of $N = 100$ monomers. Two adjacent monomers are freely connected by a segment of length b . The repulsive potential between two non-adjacent monomers is taken to be of the square wall type: $V(|\vec{r}_1 - \vec{r}_2|) = V_0$ if $|\vec{r}_1 - \vec{r}_2| \leq d$ and 0 otherwise. In the simulation, it is tacitly assumed that $V_0 \gg k_B T$. In practice, this means that the only accepted configurations are such that the distances between any pair of two non- adjacent monomers are $\geq d$. The short range potential used in our calculation corresponds to a different limit : $V_0/k_B T \rightarrow \infty$, $d \rightarrow 0$, with $\frac{4\pi}{3}d^3V_0/k_B T$ going to a finite limit γb^3 . The limiting potential $V(|\vec{r}_1 - \vec{r}_2|)$ reduces to the zero range potential $\gamma b^3 \delta(\vec{r}_1 - \vec{r}_2)$. The coupling constant λ used in our computation is to be identified with $\frac{18}{\pi^2} \gamma b^3$. Despite the difference of the two kinds of limit, we see on FIG.7 that the M.C. simulation results with $d = b$ are fairly well fitted by our HF curve, if we choose $\lambda = 0.7$. (We work in a system where b and $k_B T$ are taken respectively as units of length and energy). In physical terms, this may suggest that the shape of the force vs

extension curve is rather insensitive to the potential range d , as long as it is equal or smaller than the monomer length b . This important point could be confirmed in two ways: one by MC simulations with $d/b < 1$, second by solving numerically the HF integral equation (32), involving finite range Yukawa or exponential potentials. If this last numerical program can be achieved successfully, it will also open the road to HF method applications to biological polymer like ssDNA, using more realistic monomer-monomer potentials.

Conclusion

The exploratory investigation of the HF method, as a tool for the study of flexible self-avoiding polymers, appears encouraging enough to justify an extension of the present work in several directions. The most urgent task is perhaps to get an estimate of the "non planar" diagrams contributions to the self-consistent equation, along the lines suggested at the end of section 3.3. Despite the good agreement with the MC simulations, it is far from obvious that the main physical results of the present work stay robust vis-à-vis such corrections.

The second road to be explored is the numerical solving of the self-consistent equation (32) with more realistic monomer-monomer potential $V(r)$, say a Yukawa potential, rather than the short range limit used in the present paper. The numerical work load will not be sensibly increased if one takes for $V(r)$, a superposition of Yukawa and exponential potentials, adjusted in such a way that the monomer-monomer interactions are attractive for distance about the hydrogen bond length and become repulsive when one reaches distances in the range of the Debye length. The MC simulations and the HF model force vs extension curves deviate from the data relative to inhibited hydrogen bonding [10], in the low force regime. In particular the experimental curves suggest that the molecular chain extension vanishes for a small but finite value of the stretching force, about $0.05pN$. This could be an indication that hairpin structures are still present at very low force, say below $0.1pN$. It will be of interest to see, if by adjusting the strength of the attractive monomer-monomer interactions, our HF model is able to reproduce the data in the whole range of force.

Acknowledgments

It is a great pleasure to thank the members of the biomolecular physics group at ENS, M.-N. Dessinges, B. Maier, M. Peliti, D. Bensimon and V. Croquette, for communicating their results before publication. We are very grateful to D. Bensimon for his careful reading of the manuscript and for many judicious remarks.

References

- [1] S.B. Smith, L. Finzi and C. Bustamante, *Science* **258**, 1122 (1992).
- [2] T.T. Perkins and S.R. Quake and D.E. Smith and S. Chu, *Science* **264**, 8222 (1994).
- [3] T.R. Strick, J.-F. Allemand, D. Bensimon, A. Bensimon and V. Croquette, *Science* **271**, 1835 (1996).
- [4] C. Bustamante, J.F. Marko, E.D. Siggia and S. Smith, *Science* **265**, 1599 (1994); A. Vologodskii, *Macromolecules* **27**, 5623 (1994).
- [5] M. Fixman and J. Kovac, *J. Chem. Phys.* **58**, 1564 (1973).
- [6] C. Bouchiat, M.D. Wang, S. M. Block, J.-F. Allemand, and V. Croquette, *Biophys. J.* **76**, 409, (1999).
- [7] T.R. Strick, J.-F. Allemand, D. Bensimon, A. Bensimon and V. Croquette, *Prog. Biophys.Molec.Biol.* **74**, 57 (2000)
- [8] S. Kuznetsov, Y. Shen, A. Benigh and A. Ansari, *Biophys. J.* **81**, 2864, (2001) and references therein.
- [9] B. Maier, D. Bensimon and V. Croquette, *Proc. Natl. Acad. Sci. (USA)* **97**, 12002,(2000)
- [10] M.-N. Dessinges, B. Maier, M. Peliti, D. Bensimon and V. Croquette. Stretching single stranded DNA, a real self-avoiding and interacting heteropolymer. Preprint ENS December 2001.
- [11] A. Montanari and M. Mézard *Phys. Rev. Lett.* **86**, 2178 (2001).
- [12] A. L. Fetter and J. D. Walecka *Quantum Theory of Many-Particle Systems* (1971) MacGraw-Hill, Inc.
- [13] G. Parisi *Statistical Field Theory in Frontiers in Physics* (1988) Addison Wesley Publishing Company
- [14] T.A Vilgis *Polymer theory: paths integrals and scaling* *Physics Reports* **336** (2000) 167-254
- [15] F.J. Dyson, *Phys.Rev.* **75**,486 (1949);*Phys.Rev.* **75**,1736 (1949)
- [16] P.G. de Gennes, *Scaling Concepts in Polymers Physics*, Cornell University Press (1979).